OPEN ACCESS

University of BRISTOL

Publisher's PDF, also known as Version of record

Link to published version (if available):
10.1126/sciadv.1601667

Link to publication record in Explore Bristol Research

PDF-document

University of Bristol - Explore Bristol Research

General rights

Fully gapped superconductivity with no sign change in the prototypical heavy-fermion CeCu$_2$Si$_2$

Takuya Yamashita,[1]* Takaaki Takenaka,[2]* Yoshifumi Tokiwa,[1]* Joseph A. Wilcox,[3]*
Yuta Mizukami,[2] Daiki Terazawa,[1] Yuichi Kasahara,[1] Shunichiro Kittaka,[4] Toshiro Sakakibara,[4]
Marcin Konczykowski,[5] Silvia Seiro,[6] Hirale S. Jeevan,[6] Christoph Geibel,[6] Carsten Putzke,[3]
Takafumi Onishi,[1] Hiroaki Ikeda,[7] Antony Carrington,[3]† Takasada Shibauchi,[2]† Yuji Matsuda[1]†

In exotic superconductors, including high-T_c copper oxides, the interactions mediating electron Cooper pairing are widely considered to have a magnetic rather than a conventional electron-phonon origin. Interest in this exotic pairing was initiated by the 1979 discovery of heavy-fermion superconductivity in CeCu$_2$Si$_2$, which exhibits strong antiferromagnetic fluctuations. A hallmark of unconventional pairing by anisotropic repulsive interactions is that the superconducting energy gap changes sign as a function of the electron momentum, often leading to nodes where the gap goes to zero. We report low-temperature specific heat, thermal conductivity, and magnetic penetration depth measurements in CeCu$_2$Si$_2$, demonstrating the absence of gap nodes at any point on the Fermi surface. Moreover, electron irradiation experiments reveal that the superconductivity survives even when the electron mean free path becomes substantially shorter than the superconducting coherence length. This indicates that superconductivity is robust against impurities, implying that there is no sign change in the gap function. These results show that, contrary to long-standing belief, heavy electrons with extremely strong Coulomb repulsions can condense into a fully gapped s-wave superconducting state, which has an on-site attractive pairing interaction.

INTRODUCTION

The discovery of heavy-fermion superconductivity in CeCu$_2$Si$_2$ was an important turning point in the history of superconductivity because it led to the birth of research on non–electron-phonon–mediated pairing (1, 2). Heavy-fermion superconductivity is usually intimately related to magnetism in some form. In particular, superconductivity often occurs in the vicinity of a zero-temperature magnetic instability known as a quantum critical point (QCP) (2–4). Thus, it is widely believed that in these materials, Cooper pairing is mediated by magnetic fluctuations. The superconducting gap structure is a direct consequence of the mechanism producing the pairing. In phonon-mediated conventional superconductors with a finite on-site pairing amplitude in real space (Fig. 1A), the superconducting gap function $\Delta(\boldsymbol{k})$ is isotropic in momentum space (Fig. 1B). On the other hand, in magnetically mediated unconventional superconductors, the on-site pairing amplitude vanishes because of strong Coulomb repulsion, and superconductivity is caused by a potential that is only attractive for particular displacements between the electrons forming the Cooper pair (Fig. 1C) (5). A net attractive interaction can be realized if the superconducting gap changes sign on the Fermi surface (Fig. 1, D and E). In some materials, such as cuprates (6) and the heavy-fermion CeCoIn$_5$ (7, 8), the sign change of the gap leads to gap functions with nodes along certain momentum directions. However, in certain iron-pnictide superconductors,

the gap function has no nodes but may change sign between the well-separated electron and hole Fermi surface pockets (9, 10).

CeCu$_2$Si$_2$ is a prototypical heavy-fermion superconductor near a magnetic instability (1, 11) with a transition temperature $T_c \simeq 0.6$ K (Fig. 2A) (1). The Fermi surface consists of heavy-electron and light-hole bands (Fig. 2B) (12). Slight variations in stoichiometry lead to "A"-type and "S"-type crystals; the former is antiferromagnetic and the latter is superconducting without magnetic ordering but lying very close to a magnetic QCP (Fig. 2A). The in-plane resistivity above T_c in zero field, which follows a power law $\rho_a = \rho_{a0} + AT^\epsilon$, with $\epsilon = 1.5$ (Fig. 2C, inset), along with the heat capacity, which follows $C/T = \gamma_N - a\sqrt{T}$ in the normal state slightly above the upper critical field, are consistent with non–Fermi liquid behaviors expected for three-dimensional antiferromagnetic quantum critical fluctuations (13–15). The magnetic field–induced recovery of Fermi liquid behavior with $\epsilon = 2$ shown in Fig. 2C bears striking resemblance to other heavy-fermion compounds in the vicinity of QCPs, such as CeCoIn$_5$ and YbRh$_2$Si$_2$ (16, 17). A critical slowing down of the magnetic response, revealed by neutron scattering (18) and nuclear quadrupole resonance (NQR) (19) in the normal state, has also been attributed to antiferromagnetic fluctuations near the QCP. These results have led to a wide belief that antiferromagnetic fluctuations are responsible for the pairing interaction in CeCu$_2$Si$_2$. Here, we report a comprehensive study of the gap structure of S-type CeCu$_2$Si$_2$ using several different probes, which together are sensitive to the gap structure on all Fermi surface sheets, and also any possible changing of gap sign between sheets.

RESULTS

Specific heat

Specific heat C is a bulk probe that measures all thermally induced excitations. Figure 3A and its inset depict the specific heat divided by temperature C/T for a crystal used in the present study. At zero field, C/T exhibits a sharp transition at T_c and tends toward saturation at

[1]Department of Physics, Kyoto University, Kyoto 606-8502, Japan. [2]Department of Advanced Materials Science, University of Tokyo, Kashiwa, Chiba 277-8561, Japan. [3]H. H. Wills Physics Laboratory, University of Bristol, Bristol BS8 1TL, UK. [4]Institute for Solid State Physics, University of Tokyo, Kashiwa, Chiba 277-8581, Japan. [5]Laboratoire des Solides Irradiés, École Polytechnique, CNRS, Commissariat à l'Energie Atomique et aux Energies Alternatives, Université Paris-Saclay, 91128 Palaiseau Cedex, France. [6]Max Planck Institute for Chemical Physics of Solids, Nöthnitzer Strasse 40, 01187 Dresden, Germany. [7]Department of Physics, Ritsumeikan University, Kusatsu 525-8577, Japan.
*These authors contributed equally to this work.
†Corresponding author. Email: a.carrington@bristol.ac.uk (A.C.); shibauchi@k.u-tokyo.ac.jp (T.S.); matsuda@scphys.kyoto-u.ac.jp (Y.M.)
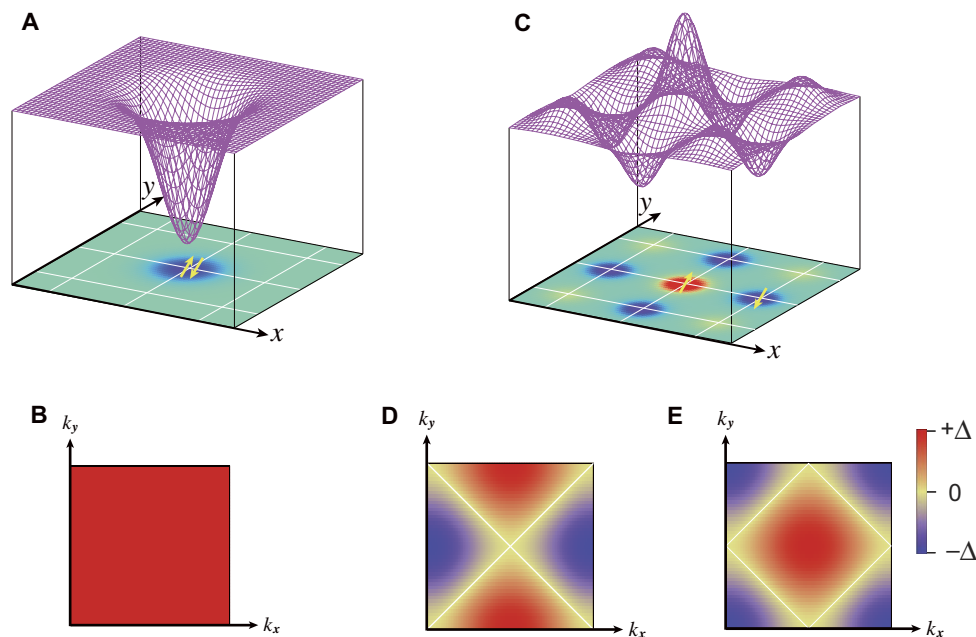
Fig. 1. Pairing interactions and superconducting gap functions. (**A**) Pairing interaction in real space for attractive force mediated by electron-phonon interaction. Blue part corresponds to attractive region. Both electrons composing the Cooper pair can occupy the same atom. (**B**) Isotropic s-wave superconducting state in the momentum space driven by the attractive force shown in (A). The gap function is constant in the entire Brillouin zone. (**C**) Pairing interaction due to magnetic fluctuations. The red and blue parts correspond to repulsive and attractive regions, respectively. Both electrons cannot occupy the same atom. Superconductivity is caused by the attractive part of the oscillating pairing interaction. (**D** and **E**) Examples for the gap structures in momentum space for unconventional superconductors caused by an on-site repulsive force, $d_{x^2-y^2}$ symmetry (D), and $s_\pm$ symmetry (E). Because of the sign change of the superconducting order parameter, the gap vanishes on the yellow lines. When the Fermi surface crosses these lines, gap nodes appear.

the lowest temperature. The C/T value at the lowest temperature, 15 mJ/K^2 mol, is less than 2% of γ_N, which indicates a very low number of quasi-particle excitations and that any inclusion of nonsuperconducting A-type material is very small. This value is around half of that previously reported (20) and demonstrates the improved quality of the present samples. The data are well fitted by an exponential T dependence, showing a lack of thermally induced excitations at the lowest temperatures in agreement with the previous studies (20, 21). A linear behavior does not fit our C/T data but if it was forced to, then a fit above 90 mK in Fig. 3A would lead to an unphysical negative intercept at $T = 0$ K. This is indicative of a fully gapped state with minimal disorder. More precisely, because the specific heat is dominated by the parts of the Fermi surface where the Fermi velocity is low (or mass is large), the C/T data suggest the absence of line nodes in the heavy electron band.

Penetration depth and lower critical field
By contrast, the magnetic penetration depth measures the surface of the sample (to a depth of a few micrometers) and is dominated by the low-mass, high-velocity parts of the Fermi surface. We find that the in-plane penetration depth $\lambda_{ab}(T)$ at low temperatures ($T \ll T_c$) exhibits strong curvature and tends toward becoming T-independent (Fig. 3B), similar to the results for C/T and in contrast to the T linear dependence, expected for clean superconductors with line nodes (22). A fit to power law T dependence $\Delta\lambda(T) = (\lambda_{ab}(T) - \lambda_{ab}(0)) \propto T^n$ gives a high power $n > 3.5$ (see section S1 and figs. S1 and S2), which is practically indistinguishable from the exponential dependence expected in fully gapped superconductors. Because λ_{ab} measures the in-plane superfluid response, our data show that gap nodes, at which quasi-particles with momentum parallel to the ab plane are excited, are absent on the light-hole bands.

For a more detailed analysis of the superconducting gap structure, the absolute value of $\lambda_{ab}(0)$ is necessary so that the normalized superfluid density $\rho_s(T) = \lambda_{ab}^2(0)/\lambda_{ab}^2(T)$ can be calculated. Unfortunately, previous measurements have reported a wide spread of values of $\lambda_{ab}(0)$ [120 to 950 nm (23, 24)], which probably reflects differences in sample stoichiometry between studies. We have estimated $\lambda_{ab}(0) = 700$ nm from Hall-probe magnetometry measurements of the lower critical field H_{c1} in the same samples, as used for our $\Delta\lambda(T)$ study (section S2 and fig. S3). The inset of Fig. 3B shows the T dependence of $\rho_s(T)$. Near T_c, we find convex curvature in $\rho_s(T)$, which is a signature frequently observed in multigap superconductors (25). Two-gap behavior has been reported in the recent scanning tunneling spectroscopy (26) and specific heat measurements (20, 21).

Thermal conductivity
Thermal conductivity is a bulk, directional probe of the quasi-particle excitations and, like penetration depth, is dominated by the high-velocity parts of the Fermi surface (27). Figure 4A and its inset show the T dependence of the in-plane thermal conductivity κ_a/T (with heat current $\mathbf{Q} \parallel a$). The thermal conductivity in the normal state at $T \to 0$ K, slightly above the upper critical field for $\mathbf{H} \parallel$ c, obeys well the Wiedemann-Franz law, $\kappa_a/T = L_0/\rho_a$ (Fig. 4A, dashed line), where L_0 is the Lorenz number and ρ_a is the in-plane resistivity. At the lowest temperatures, κ_a/T extrapolated to $T = 0$ K is zero within our experimental resolution and is at least an order of magnitude smaller than that expected for line nodes (section S3 and fig. S4), consistent with the $\lambda(T)$ results.

Further evidence for the absence of any nodes is provided by magnetic field dependence of κ. In fully gapped superconductors, where all the quasi-particle states are bound to vortex cores, the magnetic field $\mathbf{H}$
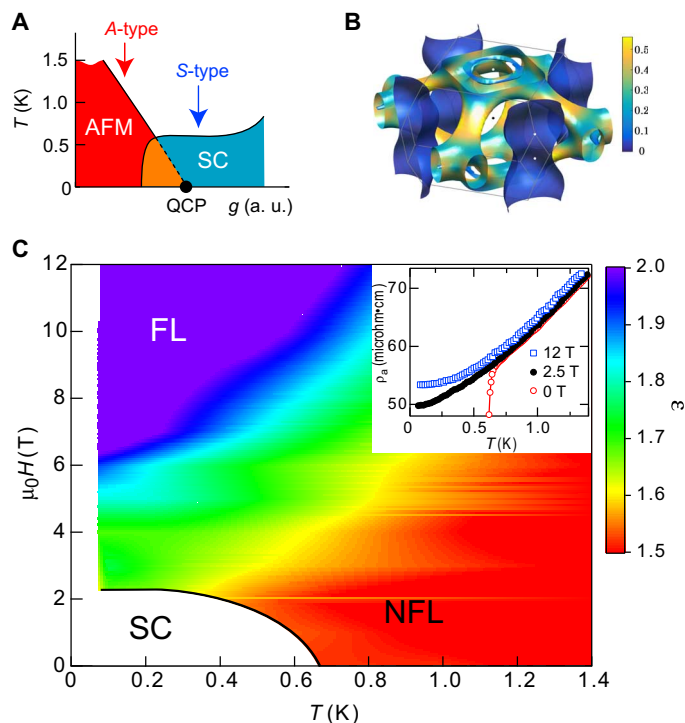
Fig. 2. Phase diagrams and electronic structure of CeCu$_2$Si$_2$. (**A**) Schematic T-g phase diagram, where g is a nonthermal control parameter, such as pressure, substitution, or Cu deficiency. Red and blue arrows indicate two different types of CeCu$_2$Si$_2$ with antiferromagnetic (A-type) and superconducting (S-type) ground states, respectively. The S-type crystal locates very close to antiferromagnetic (AFM) QCP. (**B**) Fermi surface colored by the Fermi velocity (in units of 10^6 m/s) obtained by the local density approximation (LDA) + U calculation (12). Fermi surface consists of separated electron and hole pockets: heavy electron pockets with cylindrical shape around X-point and rather complicated light hole pockets centered at Γ point. (**C**) H-T phase diagram with color coding of T exponent (ϵ) of the in-plane electrical resistivity, $\rho(T) = \rho_0 + AT^{\epsilon}$ for **H** ∥ c. Inset shows the T dependence of $\rho(T)$ in zero field and in magnetic fields of 2.5 and 12 T applied along the c axis.

hardly affects κ except in the vicinity of the upper critical field H_{c2}. By contrast, in nodal superconductors, heat transport is dominated by the delocalized quasi-particles. In the presence of a supercurrent with velocity $\mathbf{v}_s$ around the vortices, the energy of a quasi-particle with momentum $\mathbf{p}$ is Doppler-shifted relative to the superfluid by $E(\mathbf{p}) \rightarrow E(\mathbf{p}) - \mathbf{v}_s \cdot \mathbf{p}$, giving rise to an initial steep increase of $\kappa(H)/T \propto \sqrt{H}$ for line nodes and $\kappa(H)/T \propto H \log H$ for point nodes. Thermal conductivity selectively probes the quasi-particles with momentum parallel to the thermal current ($\mathbf{p} \cdot \mathbf{Q} \neq 0$) and with momentum perpendicular to the magnetic field ($\mathbf{p} \times \mathbf{H} \neq 0$) because $\mathbf{H} \perp \mathbf{v}_s$ (27). To probe the quasi-particle excitations on the whole Fermi surface, we performed measurements for three different configurations: (i) κ_a for **H** ∥ c, (ii) κ_c for **H** ∥ c, and (iii) κ_c for **H** ∥ a (Fig. 4, B and C). For (i) and (ii), thermal conductivity selectively probes the quasi-particles with in-plane momentum, whereas for (iii), it selectively probes quasi-particles with out-of-plane momentum. For configuration (ii), there is structure at $\mu_0 H \sim 1$ T, which again indicates the presence of multiple superconducting gaps. The H dependence for configuration (iii) shown in Fig. 4C is similar to configuration (i). Remarkably, in all configurations, magnetic field hardly affects the thermal conduction in the low-field regime (Fig. 4, B and C); the field-induced enhancement, $\Delta\kappa(H) \equiv \kappa(H) - \kappa(0)$ is less than $^1/_{100}$ of the normal-state value $\Delta\kappa(H_{c2})$ even at $H/H_{c2} \sim 0.15$, demonstrating a vanishingly small number of delocalized quasi-particles excited by magnetic field. As shown by the dashed lines in Fig. 4D, $\Delta\kappa(H)/\Delta\kappa(H_{c2})$ is far smaller than that expected for line and point nodes.

Electron irradiation

The above measurements of $C(T)$, $\Delta\lambda(T)$, and $\kappa(T, H)$ demonstrate the absence of any kind of nodes in the gap function on the whole Fermi surface. To further distinguish between the remaining possible gap structures, we have measured the effect of impurity-induced pair breaking on T_c. These measurements are a sensitive test of possible sign changes in the gap function either between different Fermi surface sheets or on a single sheet. Impurity-induced scattering between sign-changing areas of Fermi surface will reduce T_c very rapidly, whereas if there is no sign change, the reduction will be much slower or even zero.
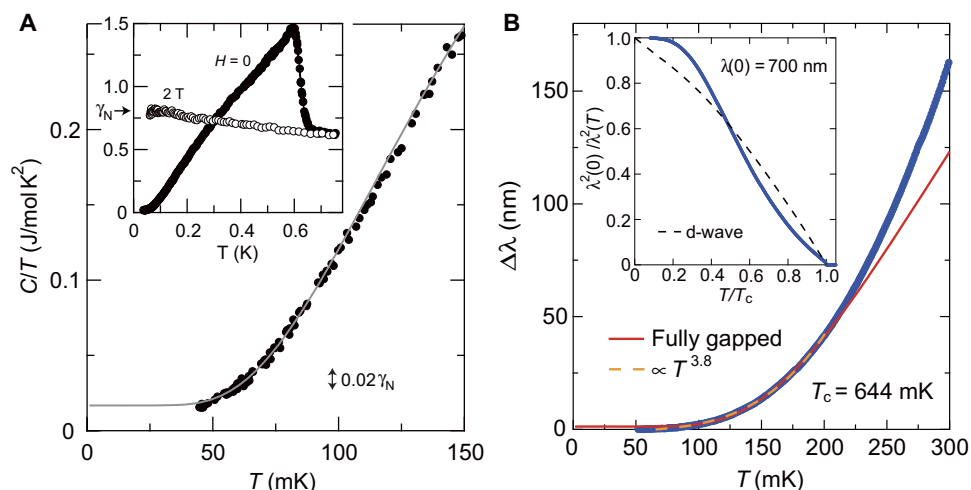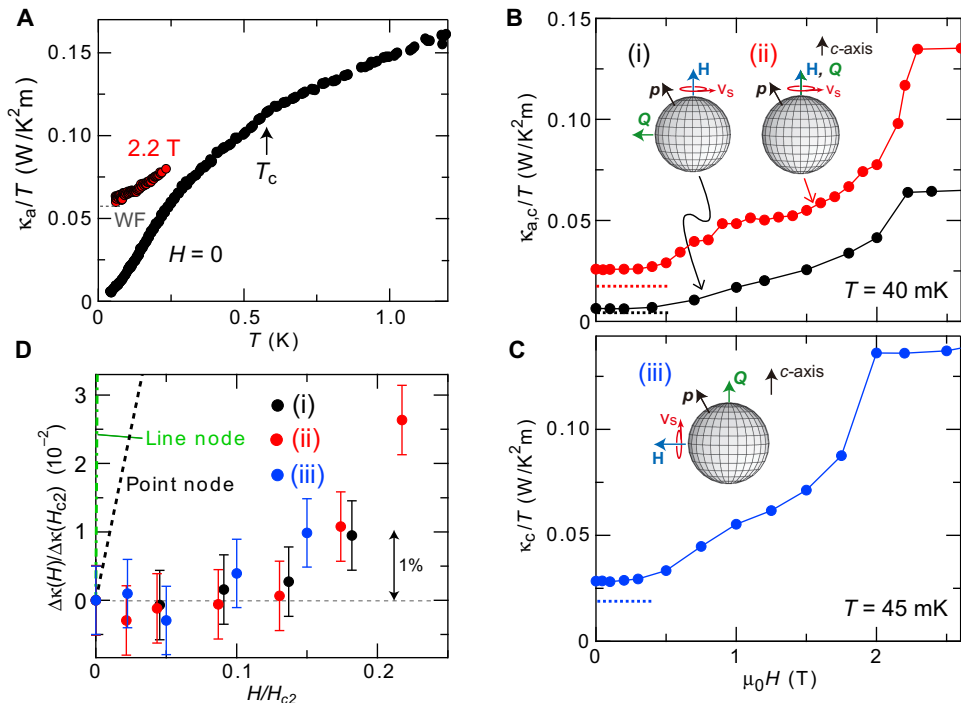

Fig. 3. Temperature dependencies of specific heat and London penetration depth well below the superconducting transition temperature T_c. (**A**) Inset shows the specific heat divided by temperature C/T in zero field and in the normal state at $\mu_0 H = 2$ T for **H** ∥ ab plane. The main panel shows C/T at low temperatures. The gray solid line is an exponential fit of the data, yielding $\Delta = 0.39$ K. (**B**) Temperature-dependent change in the in-plane penetration depth $\Delta\lambda$ in a single crystal of CeCu$_2$Si$_2$. The dashed (solid) line is a fit to a power law (exponential) temperature dependence up to 0.2 K. Inset shows the normalized superfluid density $\rho_s(T) = \lambda^2(0)/\lambda^2(T)$ as a function of T/T_c, extracted by using a value of $\lambda(0) = 700$ nm (section S2). The dashed line is the temperature dependence of $\rho_s(T)$ in the simple d-wave case.

Fig. 4. Thermal conductivity of CeCu$_2$Si$_2$ for various directions of thermal current and magnetic field. (A) Temperature dependence of the in-plane thermal conductivity divided by temperature κ_a/T in zero field and in magnetic field of $\mu_0 H = 2.2$ T applied along the c axis. WF refers to κ/T at $T \rightarrow 0$ calculated from the Wiedemann-Franz law. (B) Field dependence of κ/T for two different configurations: (i) κ_a/T (**Q** ∥ a) in **H** ∥ c and (ii) κ_c/T (**Q** ∥ c) in **H** ∥ c. In these configurations, thermal conductivity selectively probes the excited quasi-particles with in-plane momentum. The dashed horizontal lines represent the phonon contribution, κ_{ph}/T, estimated from the WF law above upper critical field (see the main text). (C) Field dependence of κ_c/T for configuration (iii), where **Q** ∥ c and **H** ∥ a. In this case, thermal conductivity selectively probes the excited quasi-particles with out-of-plane momentum. (D) Field-induced enhancement of thermal conductivity $\Delta\kappa(H) \equiv \kappa(H) - \kappa(0)$ normalized by the normal-state value, $\Delta\kappa(H)/\Delta\kappa(H_{c2})$, for the configurations (i), (ii), and (iii) plotted against the magnetic field normalized by the upper critical fields. Black and green broken lines represent the field dependencies expected for line and point nodes.

To introduce impurity scattering by homogeneous point defects in a controllable way, we used electron irradiation with an incident energy of 2.5 MeV (28), which according to our calculation of electron-scattering cross sections mainly removes Ce atoms. Electronic-structure calculations of CeCu$_2$Si$_2$ (12) show that the bands crossing the Fermi level are mainly composed of a single Ce f-manifold; therefore, removing Ce atoms by electron irradiation will act as a strong point scatterer and induce both intra- and interband impurity scattering with similar amplitude.

Our results show that T_c of CeCu$_2$Si$_2$ is decreased slowly with increasing dose (inset of Fig. 5A). The transition width remains almost unchanged after irradiation, indicating good homogeneity of the point defects. The temperature dependence of resistivity indicates that the primary effect of irradiation is the increase of temperature-independent impurity scattering with dose and that the temperature-dependent inelastic scattering remains unaffected. In- and out-of-plane residual resistivities reach $\rho_{a0} \sim 120$ microhm·cm and $\rho_{c0} \sim 110$ microhm·cm for irradiated crystals (inset of Fig. 5A). Using $\ell_j = v_F^j \lambda_j^2(0)\mu_0/\rho_{j0}$ ($j = ab$ or c), we obtain in- and out-of-plane mean free paths, $\ell_{ab} \sim 3.0$ nm and $\ell_c \sim 1.8$ nm, respectively. Here, we used averaged in-plane (out-of-plane) Fermi velocity $v_F^{ab} \sim 5800$ m/s ($v_F^c \sim 6800$ m/s) of the light-hole band, $\lambda_c(0) = \lambda_{ab}(0)(\xi_{ab}/\xi_c) = 480$ nm, where in-plane and out-of-plane coherence lengths are determined by the orbital-limited upper critical fields, $\xi_{ab} = 4.7$ nm and $\xi_c = 6.9$ nm, respectively (section S3). These mean free paths are obviously shorter than ξ_{ab} and ξ_c. For unconventional pairing symmetries, such as d-wave, superconductivity is completely suppressed at $\ell \lesssim 4\xi$. In stark contrast, T_c of CeCu$_2$Si$_2$ is still

as high as $\sim T_{c0}/2$ even for $\ell_c/\xi_c \sim 0.26$ and $\ell_{ab}/\xi_{ab} \sim 0.64$. Note that this ℓ/ξ is the upper limit value because ℓ is estimated from the penetration depth and conductivity, both of which are governed by the light bands, whereas ξ is determined by the upper critical field, which is governed by heavy bands. We also note that our electron irradiation data are semiquantitatively consistent with the oxygen irradiation results reported for thin films (29), although the initial $T_c = 0.35$ K for the pristine film is much lower than that of our single crystals. Thus, these results demonstrate that superconductivity in CeCu$_2$Si$_2$ is robust against impurities. This is also clearly seen by comparison to the d-wave superconductor CeCoIn$_5$ (30), which has comparable effective mass and carrier number. Figure 5A shows the residual resistivity dependence of T_c/T_{c0}, where T_{c0} is the transition temperature with no pair breaking. In CeCoIn$_5$, T_c is suppressed to zero in the sample with ρ_0/T_{c0} smaller than 10 microhm·cm/K (30), whereas T_c in CeCu$_2$Si$_2$ is still $\sim 50\%$ of T_{c0} even for the sample with ρ_0/T_{c0} larger than 150 microhm·cm/K, indicating that the pair-breaking effect in CeCu$_2$Si$_2$ is fundamentally different from that in CeCoIn$_5$.

Comparison to other materials (cuprates and iron pnictides) with sign-changing gaps confirms the much weaker effect of impurities in CeCu$_2$Si$_2$. In Fig. 5B, we plot the impurity-induced T_c reduction in a number of materials [CeCoIn$_5$ (30), YBa$_2$Cu$_3$O$_7$ (31), Ba(Fe$_{0.76}$Ru$_{0.24}$)$_2$As$_2$ (32), MgB$_2$ (33, 34), and YNi$_2$B$_2$C (35–37)] as a function of dimensionless scattering rate $\hbar/\tau_{imp}k_BT_{c0}$, where τ_{imp} is the impurity scattering time estimated from residual resistivity ρ_0 and the penetration depth, $\tau_{imp} = \mu_0\lambda_{ab}\lambda_c/\rho_0$. Plotting the data in this way removes the effect of
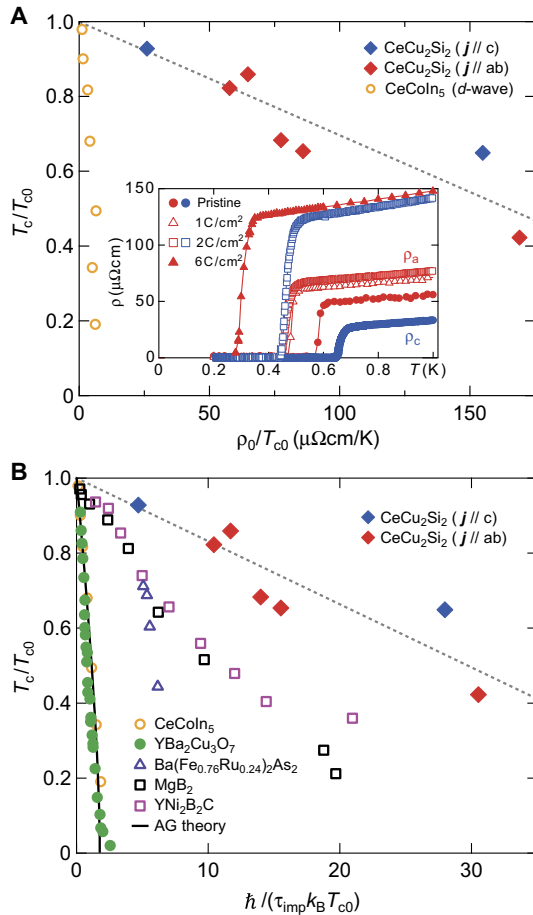
Fig. 5. Pair-breaking effect of CeCu₂Si₂. (**A**) Suppression of superconducting transition temperature T_c/T_{c0} as a function of ρ_0/T_{c0}, which is proportional to the pair-breaking parameter for CeCu₂Si₂ and Sn-substituted CeCoIn₅ (d-wave) (30). Here, T_{c0} is the transition temperature with no pair-breaking effect and ρ_0 is the residual resistivity. For CeCu₂Si₂, $T_{c0} = 0.71$ K is used. Inset shows the temperature dependence of resistivity in CeCu₂Si₂ before and after electron irradiation, which creates point defects. (**B**) Comparison of impurity effect of CeCu₂Si₂ with those of other superconductors. Suppression of superconducting transition temperature T_c/T_{c0} as a function of dimensionless pair-breaking parameter $\hbar/\tau_{imp}k_BT_{c0}$. The solid line shows the prediction of the Abrikosov-Gor'kov (AG) theory for an isotropic s-wave superconductor with magnetic impurities. We also plot the data for Sn-substituted CeCoIn₅ (d-wave) (30), electron-irradiated YBa₂-Cu₃O₇₋δ (d-wave) (31), electron-irradiated Ba(Fe₀.₇₆Ru₀.₂₄)₂As₂ (possibly $s_\pm$ wave) (32), and neutron-irradiated MgB₂ (33) and YNi₂B₂C (35). The value of T_{c0} is estimated by extrapolating two initial data points to zero $1/\tau_{imp}$ limit. Rather weak pair-breaking effect in Ba(Fe₀.₇₆Ru₀.₂₄)₂As₂ has been attributed to a large imbalance between intra- and interband scattering (32). For MgB₂ data, we use the value of $\lambda_{ab}(0) = \lambda_c(0) = 100$ nm (34). For YNi₂B₂C data, we use $\lambda_{ab}(0) = 110$ nm (36) and $\lambda_c(0) = \lambda_{ab}(0)H_{c2}^{ab}/H_{c2}^c = 140$ nm (37), where H_{c2}^{ab} and H_{c2}^c are upper critical fields parallel and perpendicular to the *ab* plane.

difference in carrier density and effective mass between the different materials, and it can be seen that the T_c reduction in CeCu₂Si₂ is much weaker than the archetypal cuprate YBa₂Cu₃O₇ (31), which has a sign-changing $d_{x^2-y^2}$ gap function. The iron pnictides present a very unusual system where the **k** dependence of the scattering is critical to the effect of impurities on T_c. Assuming that the pairing in these materials is caused by interband spin-fluctuation interactions, the gap function is expected to change sign between the electron and hole sheets ($s_\pm$ pairing). Inter-

band impurity scattering will then increase ρ_0 and decrease T_c in a similar way to other sign-changing gap materials; however, if the scattering is purely intraband, then this would increase ρ_0 but would not decrease T_c (38). It is highly unlikely that this anomalous situation could occur in CeCu₂Si₂ because the Fermi surface sheets are not well separated and, as described above, Ce vacancies would produce non–**k**-selective scattering.

The slow but finite reduction in T_c as a function of ρ_0 that we see in CeCu₂Si₂ can be explained qualitatively by the moderate gap anisotropy that we have observed in our $C(T)$ and $\lambda(T)$ measurements. In cases where there is gap anisotropy, scattering will tend to average out the gap, thus depressing T_c. However, crucially this will be at a much slower rate than for a sign-changing gap, as shown in Fig. 5B by data for the non–sign-changing s-wave superconductors MgB₂ (33) and YNi₂B₂C (35), which are known to have very anisotropic energy gaps. Our observed slower decrease in T_c as a function of impurity scattering in CeCu₂Si₂ compared to these materials is consistent with our observed moderate anisotropy.

DISCUSSION

The combination of our measurements and previous results is far more consistent with one possible gap structure. The strong reduction of the spin susceptibility in the superconducting state observed by nuclear magnetic resonance Knight shift indicates spin-singlet pairing (39), which rules out any odd-momentum (p or f) states, including those, such as the Balain-Werthamer state (40), that are fully gapped (41). This is consistent with the observation that H_{c2} is Pauli-limited (42). In the present crystal, orbital-limited upper critical fields at $T = 0$ K calculated from $H_{c2}^{orb} = -0.7T_c(dH_{c2}/dT)_{T_c}$ are 10.0 and 14.7 T for **H** ∥ *a* and **H** ∥ *c*, respectively. These values are much larger than the observed H_{c2} of 2.0 T for **H** ∥ *a* and 2.3 T for **H** ∥ *c*.

Our observation that superconductivity is robust against inter- and intraband impurity scattering rules out any sign-changing gap functions, such as d-wave or the recently proposed sign-changing $s_\pm$ state (12). Both the d-wave and $s_\pm$ states are also highly unlikely because neither could be nodeless in CeCu₂Si₂ where the electron and hole Fermi surface sheets are not well separated. Finally, unconventional states that combine irreducible representations of the gap function, such as $d_{xy} + id_{x^2-y^2}$ or $s + id_{x^2-y^2}$, can be ruled out because these states would be highly sensitive to impurities and furthermore, because in general, these representations are not degenerate, we would expect to see two distinct superconducting transitions. If there was accidental degeneracy, this would be broken by pressure or doping, but no double transitions are observed under these conditions either (11). This leads us to the surprising conclusion that the pairing in CeCu₂Si₂ is a fully gapped non–sign-changing s-wave state.

Previously, evidence for line nodes in CeCu₂Si₂ has been suggested by measurements of the NQR relaxation rate $1/T_1$ where a T^3 dependence below T_c was observed (19). However, these results would also be explained by the multigap nature of the superconductivity shown here by our $C(T)$, $\lambda(T)$, and $\kappa(H)$ measurements. The absence of the coherence (Hebel-Slichter) peak in $1/T_1(T)$ below T_c may be explained by the quasi-particle damping especially for anisotropic gap and thus does not give conclusive evidence for the sign-changing gap (21). Inelastic neutron scattering shows an enhancement of magnetic spectral weight at about $E \sim 2\Delta$ (43), which could be interpreted in terms of a spin resonance expected in superconductors with a sign-changing gap. However, this enhancement is very broad compared with some

cuprates (*44*) and CeCoIn$_5$ (*45*), therefore is not clearly a resonance peak, which is expected to be sharp in energy. Moreover, recent calculations show that a broad maximum at $E \sim 2\Delta$ appears even in superconductors without sign-changing gaps (*46*). We should add that even in the d-wave CeCoIn$_5$ case, the interpretation of the neutron peak below T_c is still controversial (*47, 48*). Hence, the NQR and neutron results do not provide conclusive evidence for a sign-changing gap structure and are not necessarily inconsistent with the results here.

At first sight, our finding that CeCu$_2$Si$_2$ has a non–sign-changing s-wave gap function casts doubt on the long-standing belief that it is a magnetically driven superconductor, despite overwhelming evidence that this compound is located near a magnetic QCP. It is unlikely that the conventional electron-phonon interaction could overcome the on-site strong Coulomb repulsive force, which enhances the effective mass to nearly 1000 times the bare electron mass, in this heavy-fermion metal, which does not have high-energy strong-coupled phonons. However, recent dynamic mean field theory calculations have shown that robust s-wave superconductivity driven by local spin fluctuations is found in solutions to the Kondo lattice model, which is commonly used to describe heavy-fermion metals (*49*). Other recent theoretical work has shown that electron-phonon coupling could be strongly enhanced near a QCP again, stabilizing s-wave superconductivity (*50*). Our results might therefore support a new type of unconventional superconductivity where the gap function is s-wave but the pairing is nevertheless driven by strong magnetic fluctuations.

MATERIALS AND METHODS

S-type single crystals of CeCu$_2$Si$_2$ were grown by the flux method (*51*). Specific heat was measured by the standard quasi-adiabatic heat pulse method. The temperature dependence of penetration depth $\lambda(T)$ was measured by using the tunnel diode oscillator technique operating at ~ 14 MHz. Weak ac magnetic field (~ 1 μT) was applied along the *c* axis, inducing screening currents in the *ab* plane. Thermal conductivity was measured by the standard steady-state method using one heater and two thermometers, with an applied temperature gradient less than 2% of the sample temperature. The contacts were made by indium solder with contact resistance much less than 0.1 ohm. We examined the effect of superconductivity of indium by applying a small magnetic field and found no discernible difference. We also measured with contacts made of silver paint with contact resistance less than 0.1 ohm and observed identical results. We measured several different crystals and obtained essentially the same results.

Electron irradiation was performed in the electron irradiation facility SIRIUS (Système d'Irradiation pour l'Innovation et les Utilisations Scientifiques) at École Polytechnique. We used electrons with an incident energy of 2.5 MeV for which the energy transfer from the impinging electron to the lattice is above the threshold energy for the formation of vacancy interstitial (Frenkel) pairs that act as point defects (*28*). To prevent the point-defect clustering, we performed irradiation at 25 K using a H$_2$ recondenser. According to the standard calculations, the penetration range for irradiated electrons with 2.5-MeV energy is as long as ~ 2.75 mm, which is much longer than the thickness of the crystals (typically 50 to 100 μm). This ensures that the point defects created by the irradiation are uniformly distributed throughout the sample thickness. Our simulations also show that for 1 C/cm^2 dose, irradiation causes about one to two vacancies per 1000 Ce atoms.

SUPPLEMENTARY MATERIALS

REFERENCES AND NOTES

1. F. Steglich, J. Aarts, C. D. Bredl, W. Lieke, D. Meschede, W. Franz, H. Schäfer, Superconductivity in the presence of strong Pauli paramagnetism: CeCu$_2$Si$_2$. *Phys. Rev. Lett.* **43**, 1892–1896 (1979).
2. C. Pfleiderer, Superconducting phases of f-electron compounds. *Rev. Mod. Phys.* **81**, 1551–1624 (2009).
3. N. D. Mathur, F. M. Grosche, S. R. Julian, I. R. Walker, D. M. Freye, R. K. W. Haselwimmer, G. G. Lonzarich, Magnetically mediated superconductivity in heavy fermion compounds. *Nature* **394**, 39–43 (1998).
4. P. Thalmerier, G. Zwicknagl, *Handbook on the Physics and Chemistry of Rare Earths* (Elsevier B.V., 2004), vol. 36.
5. D. J. Scalapino, The case for $d_{x^2-y^2}$ pairing in the cuprate superconductors. *Phys. Rep.* **250**, 329–365 (1995).
6. C. C. Tsuei, J. R. Kirtley, Pairing symmetry in cuprate superconductors. *Rev. Mod. Phys.* **72**, 969–1016 (2000).
7. K. Izawa, H. Yamaguchi, Y. Matsuda, H. Shishido, R. Settai, Y. Onuki, Angular position of nodes in the superconducting gap of quasi-2D heavy-fermion superconductor CeCoIn$_5$. *Phys. Rev. Lett.* **87**, 057002 (2001).
8. B. B. Zhou, S. Misra, E. H. da Silva Neto, P. Aynajian, R. E. Baumbach, J. D. Thompson, E. D. Bauer, A. Yazdani, Visualizing nodal heavy fermion superconductivity in CeCoIn$_5$. *Nat. Phys.* **9**, 474–479 (2013).
9. I. I. Mazin, Superconductivity gets an iron boost. *Nature* **464**, 183–186 (2010).
10. P. J. Hirschfeld, M. M. Korshunov, I. I. Mazin, Gap symmetry and structure of Fe-based superconductors. *Rep. Prog. Phys.* **74**, 124508 (2011).
11. H. Q. Yuan, F. M. Grosche, M. Deppe, C. Geibel, G. Sparn, F. Steglich, Observation of two distinct superconducting phases in CeCu$_2$Si$_2$. *Science* **302**, 2104–2107 (2003).
12. H. Ikeda, M.-T. Suzuki, R. Arita, Emergent loop-nodal $s_\pm$-wave superconductivity in CeCu$_2$Si$_2$: Similarities to the iron-based superconductors. *Phys. Rev. Lett.* **114**, 147003 (2015).
13. P. Gegenwart, C. Langhammer, C. Geibel, R. Helfrich, M. Lang, G. Sparn, F. Steglich, R. Horn, L. Donnevert, A. Link, W. Assmus, Breakup of heavy fermions on the brink of 'Phase A' in CeCu$_2$Si$_2$. *Phys. Rev. Lett.* **81**, 1501–1504 (1998).
14. L. Zhu, M. Garst, A. Rosch, Q. Si, Universally diverging Grüneisen parameter and magnetocaloric effect close to quantum critical points. *Phys. Rev. Lett.* **91**, 066404 (2003).
15. A. Rosch, Interplay of disorder and spin fluctuations in the resistivity near a quantum critical point. *Phys. Rev. Lett.* **82**, 4280–4283 (1999).
16. J. Paglione, M. A. Tanatar, D. G. Hawthorn, E. Boaknin, R. W. Hill, F. Ronning, M. Sutherland, L. Taillefer, C. Petrovic, P. C. Canfield, Field-induced quantum critical point in CeCoIn$_5$. *Phys. Rev. Lett.* **91**, 246405 (2003).
17. J. Custers, P. Gegenwart, H. Wilhelm, K. Neumaier, Y. Tokiwa, O. Trovarelli, C. Geibel, F. Steglich, C. Pépin, P. Coleman, The break-up of heavy electrons at a quantum critical point. *Nature* **424**, 524–527 (2003).
18. J. Arndt, O. Stockert, K. Schmalzl, E. Faulhaber, H. S. Jeevan, C. Geibel, W. Schmidt, M. Loewenhaupt, F. Steglich, Spin fluctuations in normal state CeCu$_2$Si$_2$ on approaching the quantum critical point. *Phys. Rev. Lett.* **106**, 246401 (2011).
19. K. Ishida, Y. Kawasaki, K. Tabuchi, K. Kashima, Y. Kitaoka, K. Asayama, C. Geibel, F. Steglich, Evolution from magnetism to unconventional superconductivity in a series of CeCu$_2$Si$_2$ compounds probed by Cu NQR. *Phys. Rev. Lett.* **82**, 5353–5356 (1999).
20. S. Kittaka, Y. Aoki, Y. Shimura, T. Sakakibara, S. Seiro, C. Geibel, F. Steglich, H. Ikeda, K. Machida, Multiband superconductivity with unexpected deficiency of nodal quasiparticles in CeCu$_2$Si$_2$. *Phys. Rev. Lett.* **112**, 067002 (2014).
21. S. Kittaka, Y. Aoki, Y. Shimura, T. Sakakibara, S. Seiro, C. Geibel, F. Steglich, Y. Tsutsumi, H. Ikeda, K. Machida, Thermodynamic study of gap structure and pair-breaking effect by magnetic field in the heavy-fermion superconductor CeCu$_2$Si$_2$. *Phys. Rev. B* **94**, 054514 (2016).
22. D. A. Bonn, W. N. Hardy, Microwave surface impedance of high temperature superconductors, in *Physical Properties of High-Temperature Superconductors*, D. M. Ginsberg, Ed. (World Scientific, 1996), vol. 5.

23. Y. J. Uemura, W. J. Kossler, B. Hitti, J. R. Kempton, H. E. Schone, X. H. Yu, C. E. Stronach, W. F. Lankford, D. R. Noakes, R. Keitel, M. Senba, J. H. Brewer, E. J. Ansaldo, Y. Oonuki, T. Komatsubara, Muon spin relaxation in CeCu$_2$Si$_2$ and muon knight shift in various heavy-fermion systems. *Hyperfine Interact.* **31**, 413–418 (1986).

24. F. Gross, B.S. Chandrasekhar, K. Andres, U. Rauchschwalbe, E. Bucher, B. Lüth, Temperature dependence of the London penetration depth in the heavy fermion superconductors CeCu$_2$Si$_2$ and UPt$_3$. *Phys. C* **153–155**, 439–440 (1988).

25. R. Prozorov, V. G. Kogan, London penetration depth in iron-based superconductors. *Rep. Prog. Phys.* **74**, 124505 (2011).

26. M. Enayat, Z. Sun, A. Maldonado, H. Suderow, S. Seiro, C. Geibel, S. Wirth, F. Steglich, P. Wahl, Superconducting gap and vortex lattice of the heavy-fermion compound CeCu$_2$Si$_2$. *Phys. Rev. B* **93**, 045123 (2016).

27. Y. Matsuda, K. Izawa, I. Vekhter, Nodal structure of unconventional superconductors probed by the angle resolved thermal transport measurements. *J. Phys. Condens. Matter* **18**, R705–R752 (2006).

28. Y. Mizukami, M. Konczykowski, Y. Kawamoto, S. Kurata, S. Kasahara, K. Hashimoto, V. Mishra, A. Kreisel, Y. Wang, P. J. Hirschfeld, Y. Matsuda, T. Shibauchi, Disorder-induced topological change of the superconducting gap structure in iron pnictides. *Nat. Commun.* **5**, 5657 (2014).

29. G. Adrian, H. Adrian, Lattice disorder effects on superconductivity and electrical resistivity of heavy-fermion CeCu$_2$Si$_2$-films. *Europhys. Lett.* **3**, 819–826 (1987).

30. E. D. Bauer, F. Ronning, C. Capan, M. J. Graf, D. Vandervelde, H. Q. Yuan, M. B. Salamon, D. J. Mixson, N. O. Moreno, S. R. Brown, J. D. Thompson, R. Movshovich, M. F. Hundley, J. L. Sarrao, P. G. Pagliuso, S. M. Kauzlarich, Thermodynamic and transport investigation of CeCoIn$_{5-x}$Sn$_x$. *Phys. Rev. B* **73**, 245109 (2006).

31. F. Rullier-Albenque, H. Alloul, R. Tourbot, Influence of pair breaking and phase fluctuations on disordered high T_c cuprate superconductors. *Phys. Rev. Lett.* **91**, 047001 (2003).

32. R. Prozorov, M. Kończykowski, M. A. Tanatar, A. Thaler, S. L. Bud'ko, P. C. Canfield, V. Mishra, P. J. Hirschfeld, Effect of electron irradiation on superconductivity in single crystals of Ba(Fe$_{1-x}$Ru$_x$)$_2$As$_2$ (x=0.24). *Phys. Rev. X* **4**, 041032 (2014).

33. M. Putti, M. Affronte, C. Ferdeghini, P. Manfrinetti, C. Tarantini, E. Lehmann, Observation of the crossover from two-gap to single-gap superconductivity through specific heat measurements in neutron-irradiated MgB$_2$. *Phys. Rev. Lett.* **96**, 077003 (2006).

34. J. D. Fletcher, A. Carrington, O. J. Taylor, S. M. Kazakov, J. Karpinski, Temperature-dependent anisotropy of the penetration depth and coherence length of MgB$_2$. *Phys. Rev. Lett.* **95**, 097005 (2005).

35. A. E. Karkin, Y. N. Akshentsev, B. N. Goshchitskii, Suppression of superconductivity in YNi$_2$B$_2$C at the atomic disordering. *JETP Lett.* **97**, 347–351 (2013).

36. T. Jacobs, B. A. Willemsen, S. Sridhar, R. Nagarajan, L. C. Gupta, Z. Hossain, C. Mazumdar, P. C. Canfield, B. K. Cho, Microwave properties of borocarbide superconductors RNi_2B_2C (R=Y,Er,Tm,Ho). *Phys. Rev. B* **52**, R7022–R7025 (1995).

37. S. C. Wimbush, L. Schultz, B. Holzapfel, Angular anisotropy of the upper critical field in YNi$_2$B$_2$C. *Physica C Supercond.* **408–410**, 83–84 (2004).

38. Y. Wang, A. Kreisel, P. J. Hirschfeld, V. Mishra, Using controlled disorder to distinguish $s_\pm$ and s_{++} gap structure in Fe-based superconductors. *Phys. Rev. B* **87**, 094504 (2013).

39. Y. Kitaoka, H. Yamada, K.-i. Ueda, Y. Kohori, Y. Kohara, Y. Oda, K. Asayama, Spin susceptibility in heavy-fermion Superconductor CeCu$_2$Si$_2$. *Jpn. J. Appl. Phys.* **26**, 1221–1222 (1987).

40. R. Balian, N. R. Werthamer, Superconductivity with pairs in a relative p wave. *Phys. Rev.* **131**, 1553–1564 (1963).

41. M. Sigrist, K. Ueda, Phenomenological theory of unconventional superconductivity. *Rev. Mod. Phys.* **63**, 239–312 (1991).

42. H. A. Vieyra, N. Oeschler, S. Seiro, H. S. Jeevan, C. Geibel, D. Parker, F. Steglich, Determination of gap symmetry from angle-dependent H_{c2} measurements on CeCu$_2$Si$_2$. *Phys. Rev. Lett.* **106**, 207001 (2011).

43. O. Stockert, J. Arndt, E. Faulhaber, C. Geibel, H. S. Jeevan, S. Kirchner, M. Loewenhaupt, K. Schmalzl, W. Schmidt, Q. Si, F. Steglich, Magnetically driven superconductivity in CeCu$_2$Si$_2$. *Nat. Phys.* **7**, 119–124 (2011).

44. B. Keimer, P. Bourges, H. F. Fong, Y. Sidis, L. P. Regnault, A. Ivanov, D. L. Milius, I. A. Aksay, G. D. Gu, N. Koshizuka, Resonant spin excitations in YBa$_2$Cu$_3$O$_{6+x}$ and Bi$_2$Sr$_2$CaCu$_2$O$_{8+\delta}$. *J. Phys. Chem. Solids* **60**, 1007–1011 (1999).

45. C. Stock, C. Broholm, J. Hudis, H. J. Kang, C. Petrovic, Spin resonance in the d-wave superconductor CeCoIn$_5$. *Phys. Rev. Lett.* **100**, 087001 (2008).

46. S. Onari, H. Kontani, Neutron-inelastic-scattering peak by dissipationless mechanism in the s^{++}-wave state in iron-based superconductors. *Phys. Rev. B* **84**, 144518 (2011).

47. A. V. Chubukov, L. P. Gor'kov, Spin resonance in three-dimensional superconductors: The case of CeCoIn$_5$. *Phys. Rev. Lett.* **101**, 147004 (2008).

48. Y. Song, J. Van Dyke, I. K. Lum, B. D. White, S. Jang, D. Yazici, L. Shu, A. Schneidewind, P. Čermák, Y. Qiu, M. B. Maple, D. K. Morr, P. Dai, Robust upward dispersion of the neutron spin resonance in the heavy fermion superconductor Ce$_{1-x}$Yb$_x$CoIn$_5$. *Nat. Commun.* **7**, 12774 (2016).

49. O. Bodensiek, R. Žitko, M. Vojta, M. Jarrell, T. Pruschke, Unconventional superconductivity from local spin fluctuations in the Kondo lattice. *Phys. Rev. Lett.* **110**, 146406 (2013).

50. R. Tazai, Y. Yamakawa, M. Tsuchiizu, H. Kontani, Functional renormalization group study of orbital fluctuation mediated superconductivity: Impact of the electron-boson coupling vertex corrections. *Phys. Rev. B* **94**, 115155 (2016).

51. S. Seiro, M. Deppe, H. Jeevan, U. Burkhardt, C. Geibel, Flux crystal growth of CeCu$_2$Si$_2$: Revealing the effect of composition. *Phys. Status Solidi B* **247**, 614–616 (2010).

52. E. H. Brandt, Irreversible magnetization of pin-free type-II superconductors. *Phys. Rev. B* **60**, 11939–11942 (1999).

53. M. Sutherland, D. G. Hawthorn, R. W. Hill, F. Ronning, S. Wakimoto, H. Zhang, C. Proust, E. Boaknin, C. Lupien, L. Taillefer, R. Liang, D. A. Bonn, W. N. Hardy, R Gagnon, N. E. Hussey, T. Kimura, M. Nohara, H. Takagi, Thermal conductivity across the phase diagram of cuprates: Low-energy quasiparticles and doping dependence of the superconducting gap. *Phys. Rev. B* **67**, 174520 (2003).

54. M. J. Graf, S.-K. Yip, J. A. Sauls, D. Rainer, Electronic thermal conductivity and the Wiedemann-Franz law for unconventional superconductors. *Phys. Rev. B* **53**, 15147–15161 (1996).

Citation: T. Yamashita, T. Takenaka, Y. Tokiwa, J. A. Wilcox, Y. Mizukami, D. Terazawa, Y. Kasahara, S. Kittaka, T. Sakakibara, M. Konczykowski, S. Seiro, H. S. Jeevan, C. Geibel, C. Putzke, T. Onishi, H. Ikeda, A. Carrington, T. Shibauchi, Y. Matsuda, Fully gapped superconductivity with no sign change in the prototypical heavy-fermion CeCu$_2$Si$_2$. *Sci. Adv.* **3**, e1601667 (2017).

Fully gapped superconductivity with no sign change in the prototypical heavy-fermion CeCu$_2$Si$_2$

Takuya Yamashita, Takaaki Takenaka, Yoshifumi Tokiwa, Joseph A. Wilcox, Yuta Mizukami, Daiki Terazawa, Yuichi Kasahara, Shunichiro Kittaka, Toshiro Sakakibara, Marcin Konczykowski, Silvia Seiro, Hirale S. Jeevan, Christoph Geibel, Carsten Putzke, Takafumi Onishi, Hiroaki Ikeda, Antony Carrington, Takasada Shibauchi and Yuji Matsuda

ARTICLE TOOLS	http://advances.sciencemag.org/content/3/6/e1601667
SUPPLEMENTARY MATERIALS	http://advances.sciencemag.org/content/suppl/2017/06/19/3.6.e1601667.DC1
REFERENCES	This article cites 52 articles, 1 of which you can access for free http://advances.sciencemag.org/content/3/6/e1601667#BIBL
PERMISSIONS	http://www.sciencemag.org/help/reprints-and-permissions

Use of this article is subject to the Terms of Service